Extensive ab initio study of the electronic states of S_2 molecule including spin-orbit coupling

Wei Xing [a] [b], Deheng Shi [a], Jinfeng Sun [a], Hui Liu [b] & Zunlue Zhu [a]

[a] College of Physics and Electronic Engineering, Henan Normal University, Xinxiang 453007, China

[b] College of Physics and Electronic Engineering, Xinyang Normal University, Xinyang 464000, China

PLEASE SCROLL DOWN FOR ARTICLE

Taylor & Francis
Taylor & Francis Group

RESEARCH ARTICLE

Extensive *ab initio* study of the electronic states of S_2 molecule including spin-orbit coupling

Wei Xing[ab], Deheng Shi[a]*, Jinfeng Sun[a], Hui Liu[b] and Zunlue Zhu[a]

[a]*College of Physics and Electronic Engineering, Henan Normal University, Xinxiang 453007, China;* [b]*College of Physics and Electronic Engineering, Xinyang Normal University, Xinyang 464000, China*

The potential energy curves (PECs) of 15 Λ-S states and 24 Ω states generated from the 13 Λ-S bound states of the S_2 molecule are investigated in detail using an *ab initio* quantum chemical method. The PECs are calculated for internuclear separations from 0.12 to 1.10 nm by the complete active space self-consistent field method, which is followed by the internally contracted multireference configuration interaction approach with the Davidson modification (MRCI + Q). The spin-orbit (SO) coupling effect is accounted for by the Breit–Pauli Hamiltonian. To discuss the effect on the energy splitting by the core-electron correlations, the all-electron basis set, cc-pCVTZ with and without 2s2p correlations, is used for the SO coupling calculations of the $A^3\Sigma_u^+$ and $B'^3\Pi_g$ Λ-S states since their measurements can be found in the literature. By comparison, the cc-pCVTZ basis set with 2s2p correlations is chosen for the SO coupling calculations of 13 Λ-S bound states. To improve the quality of PECs, core-valence correlation and scalar relativistic corrections are included. Scalar relativistic correction calculations are made using the third-order Douglas–Kroll Hamiltonian (DKH3) approximation at the level of a cc-pV5Z basis set. Core-valence correlation corrections are taken into account with a cc-pCVTZ basis set. The spectroscopic parameters of 13 Λ-S bound states and 24 Ω states are calculated. With the PECs obtained by the MRCI + Q/aug-cc-pV6Z + CV + DK + SO calculations, the SO coupling splitting energies are 379.25 cm^{-1} between the A'3 and A'2 Ω state, 83.40 cm^{-1} between the A1 and A0$^-$ Ω state and 210.91 cm^{-1} between the B'2 and B'1 Ω state, which agree well with the corresponding measurements of 383, 77.51 and 209 cm^{-1}, respectively. Moreover, other spectroscopic parameters are also in excellent agreement with the measurements. It demonstrates that the spectroscopic parameters of 24 Ω states reported here for the first time can be expected to be reliable predicted ones.

Keywords: spin-orbit coupling; potential energy curve; spectroscopic parameter; scalar relativistic correction; core-valence correlation correction

1. Introduction

The spectroscopic properties of S_2 molecule have been subject of a number of experimental and theoretical investigations for a long time. The reason is that the molecule is involved in the chemistry of planetary. For example, the molecule was observed in the UV spectra of comet IRAS-Araki-Alcock [1], comet Hyakutake [2] and comet Lee [3]. The spectroscopic emission from the S_2 was observed in Jupiter's atmosphere after the impact of the Shoemaker–Levy 9 comet [4]. Spectroscopic signatures of the molecule have been observed from cometary atmospheres [1,5,6] and dense molecular clouds [7–9]. And the molecule is also thought to play a role in the photochemistry of Venus lower atmosphere [10–12] and in the circumstellar shells of carbon-rich evolved stars [13]. In addition, S_2 molecules can also be found at various natural and industrial plasmas containing sulfur compounds.

Historically, the absorption spectra of sulfur vapor at different temperatures and pressures were observed by Graham [14] early in 1910. In the about seventy years since, a number of valence states had been characterized through detailed study of their electronic spectroscopy in the ultraviolet, visible and infrared spectral regions. Some accurate spectroscopic parameters and molecular constants reported in the literature prior to 1979 were summarized by Huber and Herzberg [15]. Of these investigations summarized by Huber and Herzberg, the spectroscopic parameters of more than 10 Λ-S states had been included, but only eight Ω states generated from the four Λ-S states ($A'^3\Delta_u$, $A^3\Sigma_u^+$, $B'^3\Pi_g$ and $B''^3\Pi_u$) were involved. Since 1979, there have been a number of experiments [9,12,16–27], in which the spectroscopic parameters of several electronic states involved here were studied. From the experiments [9,12,16–27], some spectroscopic

---

*Corresponding author. Email: scattering@sina.com.cn

and molecular properties have also been extracted. Summarizing these experimental results, we find that, (1) few spectroscopic parameters exist for the Ω states, though the spin-orbit (SO) coupling effect has been investigated by many experiments [15,16,18,28,29]. In addition, no SO coupling effect has been studied except for the $A'^3\Delta_u$, $A^3\Sigma_u^+$, $B'^3\Pi_g$ and $B''^3\Pi_u$ Λ-S states up to now; and (2) the spectroscopic parameters, in particular for the T_e, are accurately determined only for several Λ-S states (such as the $X^3\Sigma_g^-$, $a^1\Delta_g$, $b^1\Sigma_g^+$ and $B''^3\Pi_u$), though a large number of Λ-S states have been observed in experiment.

Early *ab initio* study on the molecule was reported by Swope *et al.* [30] in 1979, who made the self-consistent field (SCF) and configuration interaction (CI) calculations on the 13 low-lying Λ-S states. Theodorakopoulos *et al.* [31] in 1981 performed the *ab initio* CI study of $X^3\Sigma_g^-$, $a^1\Delta_g$ and $b^1\Sigma_g^+$ Λ-S states using the atomic orbital (AO) basis sets including *f*-type species. Hess and Buenker [32] in 1982 carried out the *ab initio* calculations of $X^3\Sigma_g^-$, $a^1\Delta_g$ and $b^1\Sigma_g^+$ Λ-S states using the multireference single- and double-excitation CI (MRD-CI) wave-functions obtained in a series of AO basis sets, and obtained some spectroscopic and molecular properties of S_2. McLean *et al.* [33] in 1983 calculated the PECs and determined some spectroscopic parameters at the basis set limit for SCF and limited CI wave functions. Raghavachari *et al.* [34] studied the structures and stabilities of sulfur clusters at the HF/6-31G* level of theory. Woon and Dunning [35] in 1994 made the benchmark calculations for the second-row diatomic molecules using the internally contracted multireference CI (MRCI) approach with the correlation-consistent basis sets. Pradhan and Partridge [36] in 1996 studied the $B^3\Sigma_u^-$-$X^3\Sigma_g^-$ and $B''^3\Pi_u$-$X^3\Sigma_g^-$ bands. Urban *et al.* [37] in 1998 performed the complete active space SCF (CASSCF) calculations followed by the second-order perturbation calculations (CASPT2) for the ground state. Kiljunen *et al.* [38] in 2000 calculated the PECs of the 13 lowest Λ-S states of the molecule. Several spectroscopic parameters were reported in these studies [34–38]. Mawhinney and Goddard [39] in 2003 used the B3LYP functional density theory and effective core potential basis set to determine the spectroscopic parameters of $X^3\Sigma_g^-$, $a^1\Delta_g$ and $b^1\Sigma_g^+$ Λ-S states. Denis [40] in 2004 calculated the R_e and ω_e of ground-state molecule by the coupled cluster theory and aug-cc-pV$(n+\mathrm{d})$Z [AV$(n+\mathrm{d})$Z] basis set. Czernek and Živný [41] in 2004 used the CCSD(T)/cc-pVQZ approach to obtain the spectroscopic parameters of S_2 and some other diatomic molecules. Recently, Karton and Martin [42] in 2010 determined the accurate spectroscopic parameters of 28 ground-state diatomic molecules by means of W4 and post-W4 theories. Summarizing these theoretical studies [30–42], we find that, (1) most of them are mainly focused on the $X^3\Sigma_g^-$, $a^1\Delta_g$ and $b^1\Sigma_g^+$ Λ-S states, and few spectroscopic parameters achieve high quality; and (2) no SO coupling effect has been calculated for any Ω states generated from any Λ-S states of S_2 molecule, though the SO coupling effect may yield important influences on the spectroscopic parameters, in particular for the T_e.

Core-valence correlation and scalar relativistic corrections have important effects on the accurate prediction of spectroscopic parameters. On the one hand, when we summarize the spectroscopic properties in the literature, we find that only one group of calculations [40] included the core-valence correlation and scalar relativistic effects, and only one group of study [39] employed the effective core potential basis set. Therefore, to improve the quality of spectroscopic parameters of Λ-S states, more theoretical work should be done; on the other hand, no spectroscopic parameters of any Ω states involved in this paper have been calculated up to date to the best of our knowledge.

The aim of the present work is to extend the spectroscopic knowledge of S_2 molecule. On the one hand, the effect on the PECs by the SO coupling will be introduced in the calculations since no energy splitting calculations have been done for any Ω states, though the SO coupling effect has been observed by a number of experiments [15,16,18,28,29]; on the other hand, extensive *ab initio* calculations of spectroscopic parameters will be made, in which the core-valence correlation and scalar relativistic corrections are included so that the spectroscopic parameters of the molecule will be determined as accurately as possible.

In the next section, we will briefly describe the theory and method, which has been discussed in detail elsewhere [43]. In Section 3, the PECs of 13 Λ-S bound states ($X^3\Sigma_g^-$, $a^1\Delta_g$, $b^1\Sigma_g^+$, $c^1\Sigma_u^-$, $A'^3\Delta_u$, $A^3\Sigma_u^+$, $B''^3\Pi_u$, $B^3\Sigma_u^-$, $B'^3\Pi_g$, $1^1\Pi_u$, $f^1\Delta_u$, $e^1\Pi_g$ and $1^1\Sigma_u^+$) and two Λ-S repulsive states ($1^5\Pi$ and $2^3\Sigma_u^+$) are investigated for internuclear separations from about 0.12 to 1.10 nm. Twenty-four Ω states generated from 13 Λ-S bound states are also studied over the present internuclear separations. The PEC calculations are performed using the CASSCF method, which is followed by the internally contracted MRCI approach [44,45] with the Davidson modification (MRCI + Q) [46,47]. The effects on the PECs by the core-valence correlation and scalar relativistic corrections are included. The effects on the energy splitting of $A^3\Sigma_u^+$ and $B'^3\Pi_g$ Λ-S states by the core-electron correlations are discussed in detail. The spectroscopic parameters are calculated for the 13 Λ-S bound states and 24 Ω states. The spectroscopic

parameters are compared with those reported in the literature. Concluding remarks are made in Section 4.

2. Theory and method

For a given molecular system, the whole Hamiltonian can be written as,

$$\hat{H} = \hat{H}^{SF} + \hat{H}^{SO}, \tag{1}$$

where $\hat{H}^{SF}$ is the spin-free Hamiltonian. It can be expressed as the non-relativistic Schrödinger operator plus Douglas–Kroll Hamiltonian. $\hat{H}^{so}$ is the SO part of Breit–Pauli Hamiltonian [43,48,49]. The Breit–Pauli SO operator $\hat{H}^{so}$ can be written in atomic units as,

$$\hat{H}^{so} = \sum_\alpha \left[\sum_i \hat{h}_\alpha(i) \cdot \hat{s}_\alpha(i) + \sum_{i \neq j} \hat{g}_\alpha(i,j) \cdot \hat{s}_\alpha(i) \right], \tag{2}$$

In Equation (2), the one-electron $\hat{h}_\alpha(i)$ and two-electron $\hat{g}_\alpha(i,j)$ SO operators are defined as,

$$\hat{h}_\alpha(i) = \frac{1}{2c^2} \sum_K \frac{Z_k[r_{iK} \times \hat{p}(i)]_\alpha}{r_{iK}^3}, \tag{3}$$

and

$$\hat{g}_\alpha(i,j) = -[2\hat{g}_{o\alpha}(i,j) + \hat{g}_{s\alpha}(i,j)], \tag{4}$$

with

$$\hat{g}_{s\alpha}(i,j) = \frac{1}{2c^2} \frac{[r_{ji} \times \hat{p}(j)_\alpha]}{r_{ij}^3}. \tag{5}$$

$$\hat{g}_{o\alpha}(i,j) = \frac{1}{2c^2} \frac{[r_{ij} \times \hat{p}(j)_\alpha]}{r_{ij}^3}, \tag{6}$$

The terms $\hat{g}_{s\alpha}(i,j) \cdot \hat{s}_\alpha(i)$ and $\hat{g}_{o\alpha}(i,j) \cdot \hat{s}_\alpha(i)$ are the spin-same-orbit and spin-other-orbit two-electron SO operators. Here, all the symbols in Equations (1)–(6) have their usual meanings.

Berning *et al.* [43] thought that the Breit–Pauli operator could be very well approximated by an effective one-electron Fock operator. By means of an effective one-electron Fock operator, they [43] have incorporated the most important two-electron contributions of the SO operator, and presented an efficient method for the calculations of Breit–Pauli SO matrix elements for internally contracted MRCI wavefunction, which has been implanted in MOLPRO 2010.1 program package [50].

The PEC calculations are made for the 13 Λ-S bound states, two Λ-S repulsive states and 24 Ω states generated from the 13 Λ-S bound states by the CASSCF approach, which is followed by the internally

contracted MRCI + Q approach [46,47]. Therefore, the CASSCF is used as the reference wavefunction for the internally contracted MRCI + Q calculations. The basis set used for the PEC calculations of all the Λ-S states is the augmented correlation-consistent polarized aug-cc-pV6Z (AV6Z) set [51]. All the calculations are made with the MOLPRO 2010.1 program package [50].

Because of a limitation of the MOLPRO program package, we must treat $D_{\infty h}$ molecules in the D_{2h} subgroup. The S_2 belongs to $D_{\infty h}$ molecular symmetry. Therefore, to make the present calculations in the MOLPRO 2010.1 program package, we must substitute the $D_{\infty h}$ symmetry with the D_{2h} point group, which can be made by orienting the S_2 molecule along the Z axis. There are eight irreducible representations, A_g, B_{3u}, B_{2u}, B_{1g}, B_{1u}, B_{2g}, B_{3g} and A_u, in the D_{2h} point group. The corresponding symmetry operations for both $D_{\infty h}$ and D_{2h} are $\Sigma_g^+ \to A_g$, $\Sigma_g^- \to B_{1g}$, $\Pi_g \to B_{2g} + B_{3g}$, $\Delta_g \to A_g + B_{1g}$, $\Sigma_u^+ \to B_{1u}$, $\Sigma_u^- \to A_u$, $\Pi_u \to B_{2u} + B_{3u}$ and $\Delta_u \to A_u + B_{1u}$, respectively. The orbitals are optimized using the CASSCF approach. The state-averaged technique is used in the CASSCF calculations except for the ground state. In the CASSCF and subsequent internally contracted MRCI and MRCI + Q calculations, eight outermost molecular orbitals (MOs) are put into the active space, including two A_g, one B_{3u}, one B_{2u}, two B_{1u}, one B_{2g} and one B_{3g} symmetry MOs. The outmost six electrons in the 3s3p shell of each S atom are placed in the active space, which consists of full valence space. That is, the twelve electrons of the S_2 are distributed into eight orbitals ($4-5\sigma_g$, $4-5\sigma_u$, $2\pi_u$ and $2\pi_g$). Therefore, this active space is referred to as CAS (12, 8). The rest of electrons in the S_2 molecule are put into the closed-shell orbitals, including three A_g, one B_{3u}, one B_{2u}, three B_{1u}, one B_{2g} and one B_{3g} symmetry MOs, which correspond to 10 orbitals in the S_2 molecule ($1-3\sigma_g$, $1-3\sigma_u$, $1\pi_u$ and $1\pi_g$). In addition, the eight electrons in the 2s2p closed shell of each S atom are used as 'core electrons' for the core-valence correlation correction calculations, while the two electrons in the 1s inner shell of each S atom are frozen. That is, when we make the core-valence correlation calculations [52], only the two 1s electrons of each S atom are frozen, which correspond to two orbitals in the S_2 molecule ($1\sigma_g$ and $1\sigma_u$). When we perform the frozen-core calculations, the ten electrons in the 1s2s2p closed-shell orbitals of each S atom are frozen, which correspond to ten orbitals in the S_2 molecule ($1-3\sigma_g$, $1-3\sigma_u$, $1\pi_u$ and $1\pi_g$). In summary, there are 28 electrons in the S_2 molecule used for the core-valence correlation calculations in this work. When we use the 18 MOs ($5A_g$, $2B_{3u}$, $2B_{2u}$, $5B_{1u}$, $2B_{2g}$ and $2B_{3g}$) to carry out the PEC calculations,

we find that the PECs are smooth over the present internuclear separation range.

To determine accurately the PECs of 13 Λ-S bound and two Λ-S repulsive states and 24 Ω states of the molecule, the point spacing intervals used here is 0.02 nm for each state, except near the equilibrium internuclear position where the point spacing is 0.002 nm. Here, the smaller step is adopted around the equilibrium separation of each state so that the properties of each PEC can be displayed more clearly. For internuclear separations from 0.12 to 1.10 nm, the obtained PEC of each state is convergent. It means that two S atoms are completely separated at 1.10 nm. The convergence of each PEC for internuclear separations from 0.12 to 1.10 nm clarifies that the dissociation energy D_e can be determined by the difference between the total energy of the S_2 at the internuclear equilibrium separation (which is obtained by fitting) and the energy sum of the two S atomic fragments at 1.10 nm.

To improve the quality of spectroscopic parameters, we include the core-valence correlation and scalar relativistic corrections into the PEC calculations. Here, the core-valence correlation correction is included using a cc-pCVTZ basis set [52]. The cc-pCVTZ basis set with the core-valence correlation and the cc-pCVTZ basis set within the frozen-core approximation are used for the present core-valence correlation contribution calculations. The difference between the two energies yields the core-valence correlation contribution (denoted as CV). Scalar relativistic effect is included using the third-order Douglas–Kroll Hamiltonian approximation (DKH3) [53–55] at the level of a cc-pV5Z basis set. That is, the cc-pV5Z-DK basis set [56] with the DKH3 approximation and the cc-pV5Z basis set [57] without the scalar relativistic corrections are used for the present calculations. The difference between the two energies produces the scalar relativistic contribution (denoted as DK).

From the PECs of 13 bound Λ-S and 24 Ω states, the spectroscopic parameters, including the excitation energy term T_e referred to the ground state, dissociation energy D_e, equilibrium internuclear separation R_e, harmonic frequency ω_e, first- and second-order anharmonic constants $\omega_e x_e$ and $\omega_e y_e$, rotation-vibration coupling constant α_e and rotational constant B_e, are obtained. In order to obtain the accurate spectroscopic parameters, the PECs of 13 bound Λ-S and 24 Ω states are fitted to an analytical form by cubic splines so that the corresponding ro-vibrational Schrödinger equation can be conveniently solved. In this paper, we solve the ro-vibrational Schrödinger equation by Numerov's method [58]. That is, the ro-vibrational constants are first determined in a direct forward manner from the analytic potential by solving the ro-vibrational

Schrödinger equation, and then the spectroscopic parameters are evaluated by fitting the first ten ro-vibrational levels obtained here.

It should be pointed out that the state-averaged technique is used in the CASSCF calculations for the twenty excited states, for which the same weight factor of 0.05 is used. The 20 states are two singlet A_g, one singlet B_{3u}, one triplet B_{3u}, one singlet B_{2u}, one triplet B_{2u}, one singlet B_{1g}, one triplet B_{1g}, two singlet B_{1u}, two triplet B_{1u}, one singlet B_{2g}, one triplet B_{2g}, one singlet B_{3g}, one triplet B_{3g}, two singlet A_u and two triplet A_u states, respectively. Of these excited states, only the 14 excited states are reported in this paper. As pointed out by Dunning *et al.* [59], in order to ensure satisfactory convergence behaviour, the $AV(n+d)Z$ basis sets should be used for the S atom. However, we use the AV6Z basis set for the present calculations. The reason is as follows. The main advantage of $AV(n+d)Z$ basis sets is that they can greatly improve the convergence behavior in extrapolating the dissociation energies, whereas we do not make such extrapolation calculations in the present work. Therefore, we do not choose the $AV(n+d)Z$ basis sets for the PEC calculations here.

3. Results and discussion

3.1. *Effect on the spectroscopic parameters by core-electron correlations*

Using the method described in Section 2, we have studied the effect on the energy splitting and T_e, R_e, ω_e and D_e by the core-electron correlations. To study the effect on the energy splitting and T_e, R_e, ω_e and D_e, we use the all-electron basis set, cc-pCVTZ [52], to make the SO coupling calculations for some selected Ω states, for which the corresponding measurements can be found in the literature [15,28,29]. For convenient comparison, we collect these T_e, R_e, ω_e and D_e results calculated by the cc-pCVTZ basis set with and without 2s2p correlations together with the available measurements [15,28,29] in Table 1.

By comparison between the spectroscopic parameters obtained by the cc-pCVTZ basis set with and without 2s2p correlations, we find that the core-electron correlations have little effect on the R_e and ω_e. For example, as demonstrated in Table 1, the core-electron correlations produce the shifts of R_e and ω_e only by 0.00001 nm and 0.01 cm^{-1} for the A′3, 0.00000 nm and 0.005 cm^{-1} for the A′2, 0.00000 nm and 0.037 cm^{-1} for the A1 and 0.00001 nm and 0.003 cm^{-1} for the A0$^-$ Ω state, respectively. Such small difference can be indeed ignored.

of 31,088.14 cm^{-1} between the ^{1}D + ^{1}S and ^{3}P + ^{3}P dissociation limit is also in line with the measurements of 31,420.4 cm^{-1} [60].

Figure 1 depicts the PECs of 13 bound and two repulsive Λ-S states determined by the MRCI + Q/AV6Z + CV + DK calculations over the internuclear separations from 0.12 to 1.10 nm. As shown in Figure 1 and Table 2, the dissociation limit of B$'^3\Pi_g$ and e$^1\Pi_g$ Λ-S states is the ^{3}P + ^{3}P, which is different from the dissociation limit $^3P_g + ^1D_g$ of B$'^3\Pi_g$ and the ^{3}P + ^{1}S of e$^1\Pi_g$ Λ-S state calculated by Kiljunen *et al.* [38]. A barrier occurs for each of the two Λ-S states in the present calculations. In detail, for the B$'^3\Pi_g$ Λ-S state, the potential barrier comes out around the internuclear separation, 0.246 nm. And the depth of the potential well is about 3334.86 cm^{-1}. For the e$^1\Pi_g$ Λ-S state, the potential barrier appears near the internuclear separation, 0.232 nm. And the depth of the potential well is about 1665.53 cm^{-1}. The two molecules, S$_2$ and O$_2$,
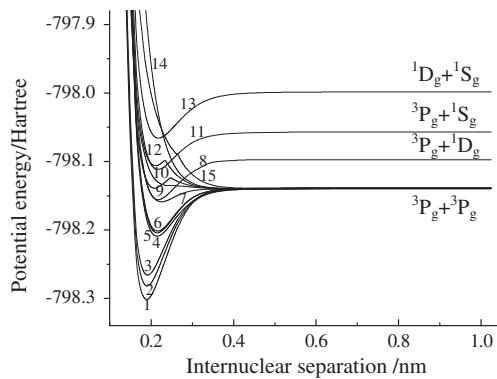

Figure 1. PECs of fifteen Λ-S states of the S$_2$ 1: X$^3\Sigma_g^-$; 2: a$^1\Delta_g$; 3: b$^1\Sigma_g^+$; 4: c$^1\Sigma_u^-$; 5: A$'^3\Delta_u$; 6: A$^3\Sigma_u^+$; 7: B$''^3\Pi_u$; 8 B$^3\Sigma_u^-$; 9: B$'^3\Pi_g$; 10: 1$^1\Pi_u$; 11: f$^1\Delta_u$; 12: e$^1\Pi_g$; 13: 1$^1\Sigma_u^+$; 14: 1$^5\Pi_u$; 15: 2$^3\Sigma_u^+$.

have the similar structure. The similar PEC shape has been observed by Takegami and Yabushita [61] for the two corresponding Λ-S states (1$^1\Pi_g$ and 1$^3\Pi_g$) of O$_2$ molecule. As shown in Figure 1, the energy at the potential well is higher than that at the dissociation limit for each of the two Λ-S states. Thus, the two Λ-S states should be very unstable and would be hard to observe. That is why Narasimham *et al.* [28] did not observe the bands of B$'^3\Pi_g$ Λ-S state arising from $v' > 0$ in their experiment. In addition, our calculations demonstrate that the dissociation limit of 1$^1\Sigma_u^+$ Λ-S state is the ^{1}D + ^{1}S, which is also different from the dissociation limit, ^{3}P + ^{1}S, reported by Kiljunen *et al.* [38].

Now we discuss the effect on the spectroscopic parameters by the core-valence correlation and scalar relativistic corrections. To simplify the discussion, here we only take the a$^1\Delta_g$ and B$''^3\Pi_u$ Λ-S states as examples at the MRCI + Q theoretical level. For convenient comparison, Table 3 collects the effect on the spectroscopic results by the core-valence correlation and/or scalar relativistic corrections. (1) The core-valence correlation correction makes the shift of T_e relatively larger by comparison with the scalar relativistic correction. Therefore, we say that the contribution to the T_e by the core-valence correlation correction is more pronounced than that by the scalar relativistic correction. (2) The core-valence correlation correction only shortens the R_e, whereas the scalar relativistic correction either shortens or lengthens it. In general, both the corrections yield the effect on the R_e, but the effect on the R_e by the core-valence correlation correction is more pronounced than that by the scalar relativistic correction. (3) The core-valence correlation raises the ω_e, but the scalar relativistic correction lowers it. And the contribution to the ω_e by the core-valence correlation correction is larger than that by the scalar relativistic correction. When we

Table 3. Effect on the spectroscopic parameters of ^{32}S$_2$ molecule by the core-valence correlation and/or relativistic corrections at the MRCI + Q/AV6Z level of theory for the a$^1\Delta_g$ and B$''^3\Pi_u$ Λ-S states.

	T_e/cm^{-1}	R_e/nm	ω_e/cm^{-1}	$\omega_e x_e$/cm^{-1}	$10^3\omega_e y_e$/cm^{-1}	B_e/cm^{-1}	$10^3\alpha_e$/cm^{-1}	D_e/eV
a$^1\Delta_g$								
MRCI + Q	4138.41	0.19070	698.512	3.128	3.08	0.28997	1.670	3.8756
CV	186.56	−0.00040	3.103	−0.017	−1.67	0.00121	0.004	0.0014
DK	−1.53	0.00003	−1.929	−0.007	0.70	−0.00008	0.002	−0.0140
CV + DK	184.58	−0.00037	1.168	−0.026	−1.24	0.00113	0.006	−0.0143
B$''^3\Pi_u$								
MRCI + Q	31,325.39	0.22689	340.626	4.399	128.9	0.20896	2.003	0.6699
CV	163.07	−0.00120	7.866	−0.914	21.0	−0.00069	−0.910	0.0156
DK	−160.21	0.00014	−0.638	−0.253	6.4	−0.00027	−0.177	0.0106
CV + DK	1.54	−0.00135	−2.778	−1.106	25.2	−0.00093	−1.071	0.0293

Table 4. Comparison of spectroscopic parameters of $^{32}S_2$ molecule determined by the MRCI + Q/AV6Z + CV + DK calculations with experimental and other theoretical results.

	T_e/cm⁻¹	R_e/nm	ω_e/cm⁻¹	$\omega_e x_e$/cm⁻¹	$10^3\omega_e y_e$/cm⁻¹	B_e/cm⁻¹	$10^3\alpha_e$/cm⁻¹	D_e/eV
$X^3\Sigma_g^-$	0.0	0.18918	724.960	2.886	15.93	0.29464	1.595	4.4090
Exp. [9]	0.0	–	–	–	–	–	4.4184 ± 0.0003(D_0)	
Exp. [15]	0.0	0.18892	725.65	2.844	–	0.29547	1.570	4.4142
Cal. [36]	0.0	0.18960	719.8	2.81	–	0.2927	1.48	4.392 ± 0.03
Cal. [40]	0.0	0.18873[a]	723.3[b]					
Cal. [42]	0.0	0.18887	727.48	2.86	–	–	1.59	
$a^1\Delta_g$	4322.99	0.19033	699.680	3.102	1.84	0.29110	1.676	3.8631
Exp. [15]	[4700][c]	0.18983	702.35	3.09	–	0.29262	1.73	
Exp. [27]	4394.25[d]	–	702.35	3.09	–	0.29262	1.73	
Cal. [31][e]	4629.62	0.1925	726					
Cal. [32][f]	–	0.195	702					
Cal. [38]	4458[d]	0.1918	684.9	3.00	–	–	–	3.741
$b^1\Sigma_g^+$	7788.72	0.19150	672.580	3.280	11.61	0.28757	1.784	3.4640
Exp. [20]	7980.99[d]	0.19115	667.	25[g]	–	0.28860	1.7845	
Cal. [38]	8001[d]	0.1931	657.6	3.31	–	–	–	3.300
$A'^3\Delta_u$	21,360.59	0.21473	490.709	2.495	25.84	0.22858	1.397	1.7641
Exp. [28]	21,356.9[d]	0.2146[h]	488.16	2.51				
$A^3\Sigma_u^+$	21,918.27	0.21550	482.794	2.590	23.29	0.22706	1.507	1.6901
Exp. [29]	21,971.4[d]	0.215	482.15	2.56	–	0.2248	1.4	
$B''^3\Pi_u$	31,326.93	0.22554	337.848	3.293	154.1	0.20803	0.932	0.6992
Exp. [18]	31,070	–	335.2	4.5	–	0.210	2.8	
Cal. [36]	31,253.97	0.22813	325.4	4.52	–	0.2026	2.61	0.516 ± 0.04
$B^3\Sigma_u^-$	31,967.36	0.21695	433.639	2.669	10.85	0.22404	1.667	1.7011
Exp. [15]	31,835	0.2170	434.0	2.75	–	0.2239	2.3	
Exp. [25]	31,832.7	–	435.2	2.72	–	0.2256	1.4	
Cal. [36]	31,826.62	0.21712	434.0	2.54	–	0.2234	1.98	1.585 ± 0.04
$f^1\Delta_u$	41,670.33	0.21651	438.222	2.703	2.50	0.22473	1.541	1.4947
Exp. [15]	[41,575.45][c]	0.21551	438.32	2.70	–	0.22704	1.78	
Cal. [38]	44,810[d]	0.2174	440.1	3.44	–	–	–	1.473

Note: [a]CCSDT/(Q, 5) + Δcore result; [b]CCSDT/(T, D) result; [c]Value in brackets is not accurate; [d]T_0 value; [e]MRD-CI with basis II of Ref. [31]; [f]MRD-CI with basis B of Ref. [32]; [g]$\Delta G_{1/2}$ value; [h]r_0 value.

analyze the T_e, R_e and ω_e results of other Λ-S states involved here, similar conclusion can also be gained. In addition, when we compare the present results with the measurements, we have found that the two corrections make these spectroscopic parameters closer to the measurements. According to these, we include the two corrections in this study so as to determine the spectroscopic parameters as accurately as possible.

With the PECs determined by the MRCI + Q/AV6Z + CV + DK calculations, we have evaluated the spectroscopic parameters of 13 Λ-S bound states by the theoretical method described in Section 2. To compare conveniently the spectroscopic results with the measurements, we collect the present spectroscopic parameters of $X^3\Sigma_g^-$, $a^1\Delta_g$, $b^1\Sigma_g^+$, $A'^3\Delta_u$, $A^3\Sigma_u^+$, $B''^3\Pi_u$, $B^3\Sigma_u^-$ and $f^1\Delta_u$ Λ-S states together with some selected

experimental [9,15,18,20,27–29] and theoretical [31,32,36,38,40,42] results in Table 4, which are these Λ-S states for which the corresponding measurements can be found in the literature. We also tabulate the present spectroscopic parameters of the rest five Λ-S bound states ($c^1\Sigma_u^-$, $B'^3\Pi_g$, $1^1\Pi_u$, $e^1\Pi_g$ and $1^1\Sigma_u^+$) in Table 5 together with some selected theoretical ones [30,38].

A number of theoretical calculations [30–42] have reported the spectroscopic parameters of the molecule in the past several decades. For length limitation of the present paper and for clarity of Table 4, we only tabulate some selected theoretical spectroscopic parameters, which can be comparable to the present ones in quality. As seen in Table 4, for the $X^3\Sigma_g^-$ Λ-S state, only the R_e results calculated by Denis [40] and

Table 5. Comparison of spectroscopic parameters of $^{32}S_2$ molecule determined by the MRCI + Q/AV6Z + CV + DK calculations with other theoretical results.

	T_e/cm^{-1}	R_e/nm	ω_e/cm^{-1}	$\omega_e x_e$/cm^{-1}	$10^2\omega_e y_e$/cm^{-1}	B_e/cm^{-1}	$10^3\alpha_e$/cm^{-1}	D_e/eV
c$^1\Sigma_u^-$	20,274.85	0.21434	488.942	2.753	8.37	0.22954	1.569	1.8973
Cal. [30]	17,900[a,b]	0.2160	489	–	–	0.2257	1.7 (CI)	
Cal. [38]	19,756[b]	0.2159	486.0	3.16	–	–	–	1.832
B$'^3\Pi_g$	35,655.85	0.20804	449.552	4.090	6.61	0.24364	2.376	3.3212
Cal. [30]	35,300[a,b]	0.2106	450	–	–	0.2375	2.3 (CI)	
Cal. [38]	35,141[b]	0.2095	439.7	4.94	–	–	–	1.067
1$^1\Pi_u$	35,499.36	0.39733	28.9794	1.830	2.46	0.66730	3.635	0.0143
Cal. [30]	37,600[a,b]	0.2243	400	–	–	0.2094	1.2 (CI)	
Cal. [38]	35,270[b]	0.245						
e$^1\Pi_g$	42,891.49	0.21043	447.342	4.553	60.37	0.23826	2.539	0.2065
Cal. [30]	43,300[a,b]	0.2143	430	–	–	0.2293 (CI)		
Cal. [38]	45,355[b]	0.2116	449.7	3.83	–	–	–	1.406
1$^1\Sigma_u^+$	51,730.61	0.21790	436.379	1.963	17.59	0.22207	1.448	1.8398
Cal. [30]	53,800[a,b]	0.2128	500	–	–	0.2326 (CI)		
Cal. [38]	44,808[b]	0.2179	436.1	3.18	–	–	–	1.473

Note: [a]obtained by the singles and doubles CI calculations with the Davidson correction; [b]T_0 value.

Karton and Martin [42] are closer to the measurements [15] than the present one. No other theoretical R_e results are closer to the measurements than the present ones except for the $X^3\Sigma_g^-$. For the ω_e, the value reported by Hess *et al.* [32] for the a$^1\Delta_g$ and the result obtained by Pradhan and Partridge [36] for the $B^3\Sigma_u^-$ Λ-S state are closer to the measurements [15,18,27] than the present ones. And for the T_e, the present results agree favorably with the measurements [15,18,20,25,27–29]. For example for the a$^1\Delta_g$ Λ-S state, only the T_e calculated by Kiljunen *et al.* [38] can be comparable with the present one in quality. For the b$^1\Sigma_g^+$, $B''^3\Pi_u$ and $B^3\Sigma_u^-$ Λ-S states, only the results obtained by Pradhan and Partridge [36] and Kiljunen *et al.* [38] are closer to the measurements [15,18,20,25] than the present ones.

As shown in Table 4, the present results are in excellent agreement with the measurements. For example, for the ground state, the deviations of the present R_e, ω_e, $\omega_e x_e$ and D_e from those [15] are only 0.00026 nm (0.14%), 0.69 cm^{-1} (0.095%), 0.04234 cm^{-1} (1.47%) and 0.0052 eV (0.12%), respectively. For the a$^1\Delta_g$ Λ-S state, the deviations of the present R_e and ω_e from those [15] are only 0.00050 nm (0.26%) and 2.67 cm^{-1} (0.39%), respectively, and the deviation of the present T_e from the measurements [27] is also only 71.26 cm^{-1}. And for the $B^3\Sigma_u^-$ Λ-S state, the deviations of the present T_e, R_e, ω_e and $\omega_e x_e$ from those [15] are only 132.36 cm^{-1} (0.42%), 0.00005 nm (0.023%), 0.361 cm^{-1} (0.08%) and 0.08089 cm^{-1} (2.94%), respectively. These comparisons indicate that the spectroscopic results obtained by the present MRCI + Q/

AV6Z + CV + DK calculations are of high quality. It should be pointed out that we collect the experimental spectroscopic parameters of A$'$2 and A1 Ω states as those of A$'^3\Delta_u$ and A$^3\Sigma_u^+$ Λ-S states for comparison in Table 4. The reasons are two-fold. One is that no accurate experimental spectroscopic parameters can be found in the literature for the two Λ-S states. The other is that the spectroscopic parameters of A$'$2 and A1 Ω states should be approximately equal to those of A$'^3\Delta_u$ and A$^3\Sigma_u^+$ Λ-S states according to our experiences.

For the five excited Λ-S states, c$^1\Sigma_u^-$, B$'^3\Pi_g$, 1$^1\Pi_u$, e$^1\Pi_g$ and 1$^1\Sigma_u^+$, no experimental spectroscopic parameters can be found, and only two groups of theoretical spectroscopic results have been reported in the literature [30,38]. The two groups of theoretical results are those reported by Swope *et al.* [30] and Kiljunen *et al.* [38], respectively. For convenient comparison, we collect the present spectroscopic parameters obtained by the MRCI + Q/AV6Z + CV + DK calculations in Table 5 together with the two groups of theoretical results [30,38]. On the one hand, the PECs of all the 13 Λ-S bound states are calculated by the same method; on the other hand, all the spectroscopic parameters are determined by the same approach. Because the spectroscopic parameters of eight Λ-S states gathered in Table 4 agree well with the measurements [9,15,18,20,27–29], we think, with reason, that the spectroscopic parameters collected in Table 5 are expected to be reliable ones. We believe that the spectroscopic parameters collected in Table 5 can be good references for the future laboratory research.

Table 6. Dissociation relationships of Ω states of S_2 calculated by the MRCI + Q/ACV5Z basis set.

Atomic state(S + S)	Ω states	Relative Energy/cm^{-1}	
		Cal.	Exp. [60]
$^3P_2 + {}^3P_2$	4, 3, 3, 2, 2, 2, 1, 1, 1, 1, 0$^+$, 0$^+$, 0$^+$, 0$^-$, 0$^-$	0	0
$^3P_2 + {}^3P_1$	3, 2, 2, 1, 1, 1, 0$^+$, 0$^-$, 0$^-$	403.19	396.8
$^3P_2 + {}^3P_0$	2, 1, 0$^+$	585.77	573.6
$^3P_1 + {}^3P_1$	2, 1, 1, 0$^+$, 0$^-$, 0$^-$	806.38	793.6
$^3P_1 + {}^3P_0$	1, 0$^+$	988.96	970.4
$^3P_0 + {}^3P_0$	0$^-$	1171.54	1147.2
$^3P_2 + {}^1D_2$	4, 3, 3, 2, 2, 2, 1, 1, 1, 1, 0$^+$, 0$^+$, 0$^+$, 0$^-$, 0$^-$	9256.09	9239.0
$^3P_1 + {}^1D_2$	3, 2, 2, 1, 1, 1, 0$^+$, 0$^-$, 0$^-$	9659.28	9635.8
$^3P_0 + {}^1D_2$	2, 1, 0$^+$	9841.86	9812.6
$^3P_2 + {}^1S_0$	2, 1, 0$^+$	21,814.90	22,181.1
$^1D_2 + {}^1S_0$	2, 1, 0$^+$	31,070.99	31,420.4

3.3. *Results and analysis of 24 Ω states*

The SO coupling effect is introduced into the present calculations by the Breit–Pauli SO operation. From that, the PECs of 24 Ω states generated from the 13 Λ-S states of S_2 molecule are calculated. For convenient discussion, we collect the dissociation relationships for the possible Ω states and their energy separations relative to the ground state ($^3P_2 + {}^3P_2$) calculated by the aug-cc-pCV5Z (ACV5Z) basis set in Table 6. In addition, we also collect the corresponding experimental values [60] in Table 6 for comparison. When the SO coupling is included, the first dissociation limit $^3P + {}^3P$ splits into the six asymptotes. As shown in Table 6, our calculated energy separations referred to the ground state agree well with the experimental values [60]. The second dissociation limit $^3P + {}^1D$ splits into the three asymptotes. Our energy separations relative to the ground state deviate from the measurements [60] by 17.09, 23.48 and 29.26 cm^{-1} for the $^3P_2 + {}^1D_2$, $^3P_1 + {}^1D_2$ and $^3P_0 + {}^1D_2$ asymptotes, respectively. As for the dissociation limit $^3P + {}^1S$ and $^1D + {}^1S$, the former splits into the $^3P_2 + {}^1S_0$, $^3P_1 + {}^1S_0$ and $^3P_0 + {}^1S_0$, and the latter splits into the $^1D_2 + {}^1S_0$, $^1D_1 + {}^1S_0$ and $^1D_0 + {}^1S_0$ asymptotes, respectively. Here we only collect the calculated separation energies of the two asymptotes, $^3P_2 + {}^1S_0$ and $^1D_2 + {}^1S_0$, in Table 6 since only the two asymptotes are involved in the present work.

The SO coupling effect causes different Λ-S states that have common Ω states to recombine. The dissociation limits of the present 24 Ω states generated from 13 Λ-S states are the $^3P_2 + {}^3P_2$ for the $X^3\Sigma_g^-(X0^+)$, $X^3\Sigma_g^-(X1)$, $A'^3\Delta_u(A'3)$, $A'^3\Delta_u(A'2)$, $A'^3\Delta_u(A'1)$, $B'^3\Pi_g(B'0^+)$, $B'^3\Pi_g(B'0^-)$, $B'^3\Pi_g(B'1)$, $B'^3\Pi_g(B'2)$, $A^3\Sigma_u^+(A1)$, $c^1\Sigma_u^-(c0^-)$ and $a^1\Delta_g(a2)$ Ω states, the $^3P_2 + {}^3P_1$ for the $B''^3\Pi_u(B''0^+)$, $B''^3\Pi_u$ $(B''0^-)$,
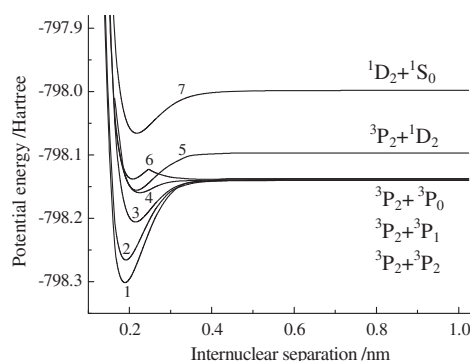

Figure 2. PECs of seven Ω states of S_2 1: $X^3\Sigma_g^-(X0^+)$; 2: $b^1\Sigma_g^+(b0^+)$; 3: $A'^3\Delta_u(A'3)$; 4: $B''^3\Pi_u(B''0^+)$; 5: $B^3\Sigma_u^-(B0^+)$; 6: $B'^3\Pi_g(B'0^+)$; 7: $1^1\Sigma_u^+(10^+)$.

$B''^3\Pi_u(B''1)$, $B''^3\Pi_u(B''2)$, $1^1\Pi_u(11)$ and $e^1\Pi_g(e1)$ Ω states, the $^3P_2 + {}^3P_0$ for the $b^1\Sigma_g^+(b0^+)$ Ω state, the $^3P_1 + {}^3P_1$ for the $A^3\Sigma_u^+(A0^-)$ Ω state, the $^3P_2 + {}^1D_2$ for the $B^3\Sigma_u^-(B0^+)$ and $B^3\Sigma_u^-(B1)$ Ω states, the $^3P_2 + {}^1S_0$ for the $f^1\Delta_u(f2)$ Ω state, the $^1D_2 + {}^1S_0$ for $1^1\Sigma_u^+(10^+)$ Ω state, respectively. The dissociation limits of 24 Ω states involved here split into seven asymptotes ($^3P_2 + {}^3P_2$, $^3P_2 + {}^3P_1$, $^3P_2 + {}^3P_0$, $^3P_1 + {}^3P_1$, $^3P_2 + {}^1D_2$, $^3P_2 + {}^1S_0$ and $^1D_2 + {}^1S_0$), of which the $^3P_2 + {}^3P_2$ is the lowest one. The PECs of 24 Ω states and their corresponding dissociation limits are shown in Figures 2–5. The PECs of A'1 and A1 Ω states almost overlap, which will make their transition spectra overlap each other and will make them hard to analyse. Due to length limitation, we do not depict the PECs of A'1 and A1 Ω states in each separate figure. For convenient discussion, we collect the spectroscopic parameters of nine Ω states generated from the three Λ-S states ($A'^3\Delta_u$, $A^3\Sigma_u^+$ and $B'^3\Pi_g$) of the molecule and their dominant Λ-S state
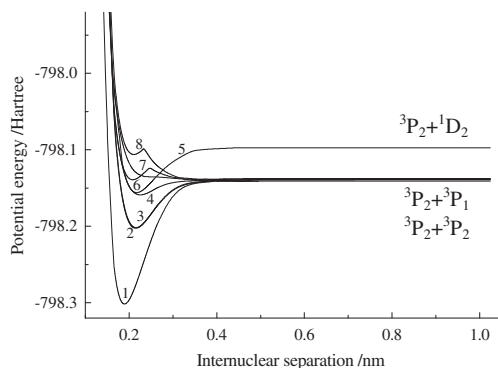
Figure 3. PECs of eight Ω states of S_2 1: $X^3\Sigma_g^-(X1)$;
2: $A'^3\Delta_u(A'1)$; 3: $A^3\Sigma_u^+(A1)$; 4: $B''^3\Pi_u(B''1)$; 5: $B^3\Sigma_u^-(B1)$;
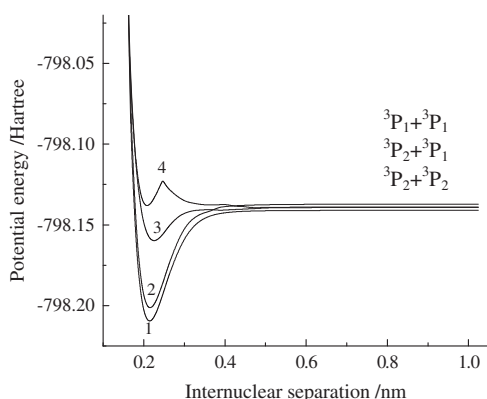6: $B'^3\Pi_g(B'1)$; 7: $1^1\Pi_u(11)$; 8: $e^1\Pi_g(e1)$.

Figure 4. PECs of four Ω states of S_2 1: $c^1\Sigma_u^-(c0^-)$;
2: $A^3\Sigma_u^+(A0^-)$; 3: $B''^3\Pi_u(B''0^-)$; 4: $B'^3\Pi_g(B'0^-)$.
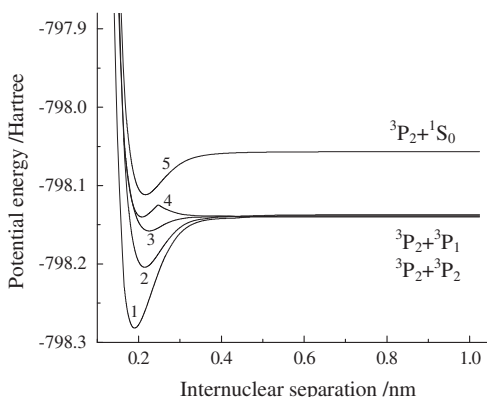

Figure 5. PECs of five Ω states of S_2 1: $a^1\Delta_g(a2)$;
2: $A'^3\Delta_u(A'2)$; 3: $B''^3\Pi_u(B''2)$; 4: $B'^3\Pi_g(B'2)$; 5: $f^1\Delta_u(f2)$.

compositions at the internuclear equilibrium separations in Table 7, for which the corresponding experimental results can be available in the literature [15,16,28,29].

The $A'^3\Delta_u$ Λ-S state splits into the three Ω states, A'3, A'2 and A'1, the spectroscopic parameters of which are almost the same as those obtained from the Λ-S state calculations. As seen in Table 7, the present R_e, ω_e and $\omega_e x_e$ of A'3 and A'2 Ω states are in excellent agreement with the measurements [15,28]. The calculated splitting energy between the A'3 and A'2 Ω state is 379.25 cm^{-1}, which is very close to the experimental vales of 383 [15] and 382.9 cm^{-1} [28]. As for the excitation energy term referred to the ground state, only the results obtained by Narasimham et al. [28] are accurate. Obviously, the present results of A'3 and A'2 Ω states are very close to them [28]. According to these, we conclude that the spectroscopic parameters of A'1 Ω state tabulated in Table 7 are reliable.

The $A^3\Sigma_u^+$ Λ-S state splits into A1 and A0$^-$ Ω states, the R_e, ω_e and $\omega_e x_e$ of which are still almost the same as those determined from the Λ-S state calculations, and are in excellent agreement with the measurements [15,25]. The deviations of the present R_e, ω_e and $\omega_e x_e$ values from the measurements [15] are 0.00059 nm (0.27%), 0.54 cm^{-1} (0.11%) and 0.00874 cm^{-1} (0.34%) for the A1 Ω state, and the deviations of the present R_e, ω_e and $\omega_e x_e$ from the experimental ones [15] are 0.00136 nm (0.64%), 0.281 cm^{-1} (0.058%) and 0.00128 cm^{-1} (0.049%), respectively, for the A0$^-$ Ω state. The present energy splitting of $A^3\Sigma_u^+$ Λ-S state is 83.40 cm^{-1}, which agrees well with the measurements of 77.51 [15] and 77.89 cm^{-1} [29].

No direct value of T_e is available for the A'3, A'2 and A'1 Ω states in the literature. Narasimham et al. [28] in 1976 estimated the T_e of A'3 Ω state by Birge–Sponer extrapolation. The corresponding result they obtained is 20,974 cm^{-1}. The energy separation between the A'3 and A'2 Ω state collected in Ref. [15] is 383 cm^{-1}. If we use such energy separation [15] and the T_e estimated in Ref. [28], we can determine the 'experimental' T_e of A'2 Ω state, 21357 cm^{-1}. The deviation of the present T_e from this result is only 28.61 cm^{-1}. In addition, the energy separations between the A'3 and A1 Ω state and between the A'3 and A0$^-$ Ω state collected in Ref. [15] are 1000.49 and 1078 cm^{-1}, respectively. Similar to the T_e of A'2 Ω state, we can calculate that the 'experimental' T_e values of A1 and A0$^-$ Ω states are 21,974.49 and 22,052 cm^{-1}, respectively. Obviously, the T_e results calculated in the present paper are in excellent agreement with the values derived here. According to these, we think that the spectroscopic parameters of A1 and A0$^-$ Ω states obtained here are accurate.

At the internuclear equilibrium separation, the dominant Λ-S state compositions of A0$^-$ Ω state are $A^3\Sigma_u^+$ (95.61%) and $c^1\Sigma_u^-$ (4.39%). With the

Table 7. Comparison of spectroscopic parameters determined by the MRCI + Q/AV6Z + CV + DK + SO calculations with the measurements for the nine Ω states generated from the three Λ-S states of $^{32}S_2$ molecule.

Ω states	T_e/cm^{-1}	R_e/nm	ω_e/cm^{-1}	$\omega_e x_e/cm^{-1}$	D_e/eV	Dominant Λ-S states at R_e (%)
A′3	21,006.36	0.21471	491.203	2.496	1.7897	$A'^3\Delta_u$(100.00)
Exp. [15]	[22,000][a]	0.2148	488.25	2.52		
Exp. [16]	21,514	–	489.5	2.7	(in solid Ne matrices)	
Exp. [28]	20,974[b]	0.2146[c]	488.23	2.52		
A′2	21,385.61	0.21473	490.709	2.495	1.7802	$A'^3\Delta_u$(100.00)
Exp. [15]	[22,383][a]	0.2148	488.16	2.51		
Exp. [16]	21,887	–	488.5	2.6	(in solid Ne matrices)	
Exp. [28]	21,356.9[b]	0.2146[c]	488.16	2.51		
A′1	21,764.64	0.21475	490.191	2.493	1.7721	$A'^3\Delta_u$(100.00)
A1	21,943.07	0.21551	482.690	2.569	1.7073	$A^3\Sigma_u^+$(100.00)
Exp. [15]	[23,000.49][a]	0.2161	482.15	2.56		
Exp. [29]	21,971.43[b]	–	482.15	2.56		
A0$^-$	22,026.47	0.21546	483.031	2.579	1.7460	$A^3\Sigma_u^+$(95.61), $c^1\Sigma_u^-$(4.39)
Exp. [15]	[23,078][a]	0.2141	482.75	2.58		
Exp. [29]	22,049.32[b]	–	482.75	2.58		
B′2	35,464.25	0.20804	449.614	4.103	3.4699	$B'^3\Pi_g$(99.99)
Exp. [15]	[36,295][a]	[0.2078][a]	[533.7][a]			
Exp. [28]	35,292.07[b]	–	[500][a]			
B′1	35,675.16	0.20804	449.594	4.098	3.3123	$B'^3\Pi_g$(99.89), $e^1\Pi_g$(0.1)
Exp. [15]	[36,504][a]	[0.2078][a]	[533.7][a]			
Exp. [28]	35,501.27[b]	–	[500][a]			
B′0$^+$	35,900.12	0.20804	449.519	4.099	3.1817	$B'^3\Pi_g$(100.00)
B′0$^-$	35,905.39	0.20804	449.479	4.081	3.1522	$B'^3\Pi_g$(99.98)

Note: [a]value in brackets is not accurate; [b]T_0 value; [c]r_0 value.

internuclear separation increased, the contribution to the energy of A0$^-$ Ω state by the $A^3\Sigma_u^+$ Λ-S state becomes less and less. For example, the dominant Λ-S state compositions are $A^3\Sigma_u^+$(35.86%), $c^1\Sigma_u^-$ (29.47%) and $B''^3\Pi_u$(34.67%) at the internuclear separation $r = 0.384$ nm, respectively. At the dissociation limit, the relative energy of A0$^-$ Ω state is higher than that of B″0$^-$ Ω state. According to our calculations, the dissociation limit of B″0$^-$ Ω state is the $^3P_2 + {}^3P_1$. Therefore, we consider that the dissociation limit of A0$^-$ Ω state should be $^3P_1 + {}^3P_1$, which is different from the one given by Frederix *et al.* [9].

Table 7 also tabulates the spectroscopic parameters of four Ω states generated from the $B'^3\Pi_g$ Λ-S state. As demonstrated in Table 7, the energy separation between the B′2 and B′1 Ω state is 210.91 cm^{-1}, which is in excellent agreement with the experimental values of 209 [15] and 209.20 cm^{-1} [28]. According to this, we think, with reason, that the energy separation of 224.96 cm^{-1} between the B′1 and B′0$^+$ Ω state and the energy separation of 5.27 cm^{-1} between the B′0$^+$ and B′0$^-$ Ω state should be accurate. The T_e values of B′2 and B′1 Ω states collected in Ref. [15] are the estimated ones, and the results measured in Ref. [28] are only T_0. Therefore, we cannot directly make the comparison between them. As for the R_e, ω_e and $\omega_e x_e$,

only the estimated experimental values can be found for the B′2 and B′1 Ω states. The present R_e are in line with the estimated ones collected in Ref. [15]. And the present ω_e are also in close to the estimated values given in Ref. [28].

The spectroscopic parameters of fifteen Ω states generated from the ten Λ-S states ($X^3\Sigma_g^-$, $a^1\Delta_g$, $b^1\Sigma_g^+$, $c^1\Sigma_u^-$, $B''^3\Pi_u$, $B^3\Sigma_u^-$, $1^1\Pi_u$, $f^1\Delta_u$, $e^1\Pi_g$ and $1^1\Sigma_u^+$) are collected in Table 8, for which no experimental spectroscopic results can be used for comparison. The present splitting energies are only 22.61 and 0.88 cm^{-1} for the $X^3\Sigma_g^-$ and $B^3\Sigma_u^-$ Λ-S states, respectively. Similar to the computed result of corresponding Λ-S state, the 11 Ω state generated from the $1^1\Pi_u$ Λ-S state has a rather shallow potential well. Therefore, this state is very unstable and hard to observe.

4. Conclusions

The PECs of fifteen Λ-S states and 24 Ω states generated from the 13 Λ-S states of the S_2 molecule are studied in detail. The internally contracted MRCI + Q method in combination with the AV6Z basis set is used to produce the PECs of fifteen Λ-S states. In order to obtain more reliable PECs, core-valence correlation

Table 8. Spectroscopic parameters of the fifteen Ω states generated from the ten Λ-S states of $^{32}S_2$ molecule obtained by the MRCI + Q/AV6Z + CV + DK + SO calculations.

Ω states	T_e/cm^{-1}	R_e/nm	ω_e/cm^{-1}	$\omega_e x_e$/cm^{-1}	D_e/eV	Dominant Λ-S states at R_e (%)
X0$^+$	0	0.18919	724.816	2.891	4.4710	X$^3\Sigma_g^-$(99.71), b$^1\Sigma_g^+$(0.28)
X1	22.61	0.18918	724.964	2.887	4.4226	X$^3\Sigma_g^-$(99.99)
a2	4345.38	0.19033	699.671	3.102	3.8907	a$^1\Delta_g$(99.99)
b0$^+$	7833.93	0.19149	672.755	3.277	3.4239	b$^1\Sigma_g^+$(99.70), X$^3\Sigma_g^-$(0.29)
c0$^-$	20,192.11	0.21438	488.580	2.748	1.8641	c$^1\Sigma_u^-$(95.72), A$^3\Sigma_u^-$(4.28)
B''0$^-$	31,144.11	0.22531	332.233	1.495	0.6970	B''$^3\Pi_u$(99.18), B$^3\Sigma_u^-$(0.81)
B''0$^+$	31,157.72	0.22538	333.482	1.630	0.6919	B''$^3\Pi_u$(100.00)
B''1	31,337.25	0.22550	336.591	3.178	0.6856	B''$^3\Pi_u$(99.37), B$^3\Sigma_u^-$(0.47), c$^1\Sigma_u^-$(0.16)
B''2	31,545.31	0.22570	340.620	4.642	0.6874	B''$^3\Pi_u$(100.00)
B0$^+$	31,995.45	0.21699	433.384	2.577	1.7016	B$^3\Sigma_u^-$(98.97), B''$^3\Pi_u$(0.96), $^1\Sigma_u^+$(0.04)
B1	31,996.33	0.21699	433.383	2.605	1.7015	B$^3\Sigma_u^-$(99.36), B''$^3\Pi_u$(0.59), 1$^1\Pi_u$(0.05)
11	36,499.95	0.45085	241.047	1.391	0.0248	1$^1\Pi_u$(42.16), B''$^3\Pi_u$(23.90), A'$^3\Delta_u$ (2.62), A$^3\Sigma_u^+$(31.31)
f2	41,696.23	0.21651	438.205	2.703	1.4946	f$^1\Delta_u$(99.99)
e1	42,924.41	0.21043	447.274	4.533	0.2059	e$^1\Pi_g$(99.89), B'$^3\Pi_g$(0.10)
10$^+$	51,764.85	0.21790	436.361	1.971	1.8392	1$^1\Sigma_u^+$(99.95), B$^3\Sigma_u^-$(0.05)

and scalar relativistic corrections are taken into account in the present work. Core-valence correlation corrections are included by a cc-pCVTZ basis set. Scalar relativistic correction calculations are performed using the DKH3 approximation at the level of a cc-pV5Z basis set. The effects on the PECs by the SO coupling are treated by the Breit-Pauli Hamiltonian. With the PECs obtained by the MRCI + Q/ AV6Z + CV + DK calculations, the spectroscopic parameters of 13 Λ-S bound states are calculated. With the PECs including the core-valence correlation and scalar relativistic corrections, the spectroscopic parameters of 24 Ω states are determined. The effects on the spectroscopic parameters of a$^1\Delta_g$ and B''$^3\Pi_u$ Λ-S states by the core-valence correlation and scalar relativistic corrections are discussed in detail. In general, core-valence correlation and scalar relativistic corrections make the spectroscopic parameters closer to the measurements. The present spectroscopic parameters well reproduce the available experimental values. The effect on the energy splitting by the core-electron correlations is studied by using the all-electron basis set, cc-pCVTZ with and without 2s2p correlations. The results illustrate that the core-electron correlations enlarge the energy splitting of the present Λ-S states, and make the energy separations closer to the available experimental ones. The spectroscopic parameters of 13 Λ-S bound states and 24 Ω states are expected to be reliable ones. We have reason to believe that the spectroscopic parameters of f$^1\Delta_u$, c$^1\Sigma_u^-$, B'$^3\Pi_g$, 1$^1\Pi_u$, e$^1\Pi_g$ and 1$^1\Sigma_u^+$ Λ-S states and all the 24 Ω states

reported here should be good references for the future laboratory research.

References

[1] M.F. A'Hearn, P.D. Feldman and D.G. Schleicher, Astrophys. J. **274**, L99 (1983).
[2] S.A. Budzien and P.D. Feldman, Icarus **99**, 143 (1992).
[3] C.M. Andreazza and E.P. Marinho, Astrophys. J. **624**, 1121, and references therein (2005).
[4] K.S. Noll, M.A. McGrath, L.M. Trafton, S.K. Atreya, J.J. Caldwell, H.A. Weaver, R.V. Yelle, C. Barnet and S. Edgington, Science **267**, 1307 (1995).
[5] R.J.A. Grim and J.M. Greenberg, Astron. Astrophys. **181**, 155 (1987).
[6] S.J. Kim, M.F. A'Hearn and S.M. Larson, Icarus **87**, 440 (1990).
[7] H.S. Liszt, Astrophys. J. **219**, 454 (1978).
[8] G.F. Mitchell, Astrophys. J. **287**, 665 (1984).
[9] P.W.J.M. Frederix, C.-H. Yang, G.C. Groenenboom, D.H. Parker, K. Alnama, C.M. Western and A.J. Orr-Ewing, J. Phys. Chem. A **113**, 14995, and references therein (2009).

[10] J.S. Lewis and F.A. Kreimendahl, Icarus **42**, 330 (1980).

[11] M.Y. Zolotov, Lunar Planet. Sci. **16**, 942 (1985).

[12] I. Shnitko, J. Fulara, I. Garkusha, A. Nagy and J.P. Maier, Chem. Phys. **346**, 8, and references herein (2008).

[13] A.E. Glassgold, Annu. Rev. Astron. Astrophys. **34**, 241 (1996).

[14] J.I. Graham, Proc. R. Soc. London Ser. A **84**, 311 (1910).

[15] K.P. Huber and G. Herzberg, *Molecular Spectra and Molecular Structure IV*, *Constants of Diatomic Molecules* (Van Nostrand, New York, 1979), and references therein.

[16] V.E. Bondybey and J.H. English, J. Chem. Phys. **72**, 3113 (1980).

[17] D.A. Peterson and L.A. Schlie, J. Chem. Phys. **73**, 1551 (1980).

[18] P. Patiño and R.F. Barrow, J. Chem. Soc., Faraday Trans. **278**, 1271 (1982).

[19] Y. Matsumi, T. Munakata and T. Kasuya, J. Chem. Phys. **81**, 1108 (1984).

[20] E.H. Fink, H. Kruse and D.A. Ramsay, J. Mol. Spectrosc. **119**, 377, (1986).

[21] C.L. Liao and C.Y. Ng, J. Chem. Phys. **84**, 778 (1986).

[22] E.H. Fink, H. Kruse, K.D. Setzer, D.A. Ramsay and M. Vervloet, Acta Phys. Hungarica **67**, 67 (1990).

[23] M.E. Green and C.M. Western, J. Chem. Phys. **104**, 848 (1996).

[24] M.E. Green and C.M. Western, J. Chem. Soc., Faraday Trans. **93**, 365 (1997).

[25] M.D. Wheeler, S.M. Newman and A.J. Orr-Ewing, J. Chem. Phys. **108**, 6594 (1998).

[26] V.I. Gerasimova, A.O. Rybaltovskii, P.V. Chernov and G. Zimmerer, Glass Phys. Chem. **28**, 59 (2002).

[27] K.D. Setzer, M. Kalb and E.H. Fink, J. Mol. Spectrosc. **221**, 127 (2003).

[28] N.A. Narasimham, V. Sethuraman and K.V.S.R. Apparao, J. Mol. Spectrosc. **59**, 142 (1976).

[29] N.A. Narasimham, K.V.S.R. Apparao and T.K. Balasubramanian, J. Mol. Spectrosc. **59**, 244 (1976).

[30] W.C. Swope, Y.-P. Lee and H.F. Schaefer III, J. Chem. Phys. **70**, 947 (1979).

[31] G. Theodorakopoulos, S.D. Peyerimhoff and R.J. Buenker, Chem. Phys. Lett. **81**, 413 (1981).

[32] B.A. Hess, R.J. Buenker, C.M. Marian and S.D. Peyerimhoff, Chem. Phys. **71**, 79 (1982).

[33] A.D. McLean, B. Liu and G.S. Chandler, J. Chem. Phys. **80**, 5130 (1984).

[34] K. Raghavachari, C.M. Rohlfing and J.S. Binkley, J. Chem. Phys. **93**, 5862 (1990).

[35] D.E. Woon and T.H. Dunning, J. Chem. Phys. **101**, 8877 (1994).

[36] A.D. Pradhan and H. Partridge, Chem. Phys. Lett. **255**, 163, (1996).

[37] M. Urban, G.H.F. Diercksen and M. Juřek, Mol. Phys. **94**, 199 (1998).

[38] T. Kiljunen, J. Eloranta, H. Kunttu, L. Khriachtchev, M. Pettersson and M. Räsänen, J. Chem. Phys. **112**, 7475 (2000).

[39] R.C. Mawhinney and J.D. Goddard, Inorg. Chem. **42**, 6323 (2003).

[40] P.A. Denis, J. Phys. Chem. A **108**, 11092 (2004).

[41] J. Czernek and O. Živný, Chem. Phys. **303**, 137 (2004).

[42] A. Karton and J.M.L. Martin, J. Chem. Phys. **133**, 144102 (2010).

[43] A. Berning, M. Schweizer, H.-J. Werner, P.J. Knowles and P. Palmieri, Mol. Phys. **98**, 1823 (2000).

[44] H.-J. Werner and P.J. Knowles, J. Chem. Phys. **89**, 5803 (1988).

[45] P.J. Knowles and H.-J. Werner, Chem. Phys. Lett. **145**, 514 (1988).

[46] S.R. Langhoff and E.R. Davidson, Int. J. Quantum Chem. **8**, 61 (1974).

[47] A. Richartz, R.J. Buenker and S.D. Peyerimhoff, Chem. Phys. **28**, 305 (1978).

[48] H.A. Bethe and E. Salpeter, *Quantum Mechanics of One- and Two-Electron Atoms* (Springer-Verlag, Berlin, 1977).

[49] S.R. Langhoff and C.W. Kern, *Modern Theoretical Chemistry* (Plenum Press, New York, 1977).

[50] MOLPRO 2010.1 is a package of *ab initio* programs written by H.-J. Werner, P.J. Knowles, R. Lindh, F.R. Manby, M. Schütz, P. Celani, T. Korona, A. Mitrushenkov, G. Rauhut, T.B. Adler, R.D. Amos, A. Bernhardsson, A. Berning, D.L. Cooper, M. J.O. Deegan, A.J. Dobbyn, F. Eckert, E. Goll, C. Hampel, G. Hetzer, T. Hrenar, G. Knizia, C. Köppl, Y. Liu, A.W. Lloyd, R.A. Mata, A.J. May, S.J. McNicholas, W. Meyer, M.E. Mura, A. Nicklass, P. Palmieri, K. Pflüger, R. Pitzer, M. Reiher, U. Schumann, H. Stoll, A.J. Stone, R. Tarroni, T. Thorsteinsson, M. Wang and A. Wolf, see http://www.molpro.net

[51] T.V. Mourik, A.K. Wilson and T.H. Dunning, Mol. Phys. **96**, 529 (1999).

[52] K.A. Peterson and T.H. Dunning, J. Chem. Phys. **117**, 10548 (2002).

[53] M. Reiher and A. Wolf, J. Chem. Phys. **121**, 2037 (2004).

[54] A. Wolf, M. Reiher and B.A. Hess, J. Chem. Phys. **117**, 9215 (2002).

[55] S. Hirata, T. Yanai, W.A. de Jong, T. Nakajima and K. Hirao, J. Chem. Phys. **120**, 3297 (2004).

[56] W.A. de Jong, R.J. Harrison and D.A. Dixon, J. Chem. Phys. **114**, 48 (2001).

[57] D.E. Woon and T.H. Dunning, J. Chem. Phys. **99**, 1914 (1993).

[58] J.L.M.Q. González and D. Thompson, Comput. Phys. **11**, 514 (1997).

[59] T.H. Dunning, K.A. Peterson and A.K. Wilson, J. Chem. Phys. **114**, 9244 (2001).

[60] C.E. Moore, Atomic energy levels, Vol.1 (Nat. Stand. Ref. Data Ser., Nat. Bur. Stand., Washington, 1971), and references therein.

[61] R. Takegami and S. Yabushita, J. Mol. Spectrosc. **229**, 63 (2005).